Nuclear mechanosensing controls MSC osteogenic potential through HDAC epigenetic remodeling

Anouk R. Killaars[a,b], Cierra J. Walker[a,b], and Kristi S. Anseth[b,c,1]

[a]Materials Science and Engineering Program, University of Colorado Boulder, Boulder, CO 80303; [b]BioFrontiers Institute, University of Colorado Boulder, Boulder, CO 80303; and [c]Department of Chemical and Biological Engineering, University of Colorado Boulder, Boulder, CO 80303

Contributed by Kristi S. Anseth, July 20, 2020 (sent for review April 9, 2020; reviewed by Charles A. Gersbach and Kris A. Kilian)

Cells sense mechanical cues from the extracellular matrix to regulate cellular behavior and maintain tissue homeostasis. The nucleus has been implicated as a key mechanosensor and can directly influence chromatin organization, epigenetic modifications, and gene expression. Dysregulation of nuclear mechanosensing has been implicated in several diseases, including bone degeneration. Here, we exploit photostiffening hydrogels to manipulate nuclear mechanosensing in human mesenchymal stem cells (hMSCs) in vitro. Results show that hMSCs respond to matrix stiffening by increasing nuclear tension and causing an increase in histone acetylation via deactivation of histone deacetylases (HDACs). This ultimately induces osteogenic fate commitment. Disrupting nuclear mechanosensing by disconnecting the nucleus from the cytoskeleton up-regulates HDACs and prevents osteogenesis. Resetting HDAC activity back to healthy levels rescues the epigenetic and osteogenic response in hMSCs with pathological nuclear mechanosensing. Notably, bone from patients with osteoarthritis displays similar defective nuclear mechanosensing. Collectively, our results reveal that nuclear mechanosensing controls hMSC osteogenic potential mediated by HDAC epigenetic remodeling and that this cellular mechanism is likely relevant to bone-related diseases.

hMSCs | epigenetic remodeling | phototunable hydrogels

The extracellular matrix (ECM) is highly dynamic and maintains tissue homeostasis by presenting a complex milieu of chemical and physical signals to cells residing in this matrix (1). Cells convey these physical signals to their internal chemical machinery via mechanotransduction pathways, which can regulate key cellular behavior such as proliferation and differentiation (2–6). Apart from biochemical signaling, recent studies demonstrate that the nucleus can act as a direct mechanosensor by undergoing deformation in the presence of mechanical forces, leading to changes in the nuclear envelope structure and composition (7–9). This structural deformation can subsequently alter chromatin organization, epigenetic modifications, and gene expression (10–12). However, the mechanisms behind remodeling of the chromatin architecture and epigenetic landscape through nuclear mechanosensing remain elusive.

Dysregulation of nuclear mechanosensing has been linked to several diseases (13). Apart from well-studied conditions, such as Hutchinson–Gilford syndrome (progeria) and cardiomyopathies (14), dysregulation of nuclear mechanosensing has been recently implicated in bone-specific diseases, such as osteoporosis, osteoarthritis, and cancer cell metastasis to bone (15–17). However, it is unclear how disruption of nuclear mechanosensing exacerbates these bone-specific diseases, so, in this study, we investigate mechanosensing in human mesenchymal stem cells (hMSCs), critical cells in the bone healing process.

Previous studies have shown that epigenetic remodeling is important in precise regulation of gene expression of hMSCs in bone development and remodeling (13, 18, 19). It has been suggested that perturbation of epigenetic programs, leading to changes in histone acetylation landscapes and chromatin structure, can affect the function and activity of hMSCs and contributes to pathologies defined by bone loss (osteoporosis, osteoarthritis) (15, 20). We previously demonstrated the role of mechanical cues in controlling hMSC epigenetic programming, linking persistent chromatin remodeling to mechanical memory induced by long-term culture on stiff hydrogel substrates (19). However, it is not yet established whether this remodeling is through 1) direct physical signaling to the nucleus and increasing chromatin accessibility, 2) up-regulation of epigenetic remodelers, such as histone deacetylases (HDACs) or histone acetyltransferases, or 3) an interplay between the two pathways.

Motivated by these questions, experiments were designed to examine the role of tension during mechanotransduction on epigenetic remodeling and osteogenesis. Previous work has relied on hydrogels with tunable initial mechanical properties, and, while these materials allow characterization of some aspects of mechanosensing, one cannot investigate the kinetics or sequence of events playing a role in nuclear mechanotransduction. To achieve this, we used a hydrogel substrate that is able to stiffen on demand, specifically, a polyethylene glycol (PEG)-based hydrogel formed by a strain-promoted azide/alkyne cycloaddition (SPAAC) reaction between azide and dibenzocyclooctyne (DBCO) groups (21). While the initial hydrogel formation proceeds rapidly and spontaneously at ambient conditions, we found that, if the initial hydrogel formulation contains excess DBCO groups, these groups can undergo a secondary cross-linking reaction in the presence of cytocompatible light irradiation (22), enabling in situ stiffening of hydrogels in the presence of cells. With this system, the initiation of nuclear mechanotransduction can be precisely controlled upon

Significance

The extracellular matrix is highly dynamic and presents mechanical signals to the residing cells to maintain tissue homeostasis. Recently, the nucleus has been implicated to be a direct mechanosensor, and dysregulation of nuclear mechanosensing might be involved in several diseases, including bone degeneration. To better understand mechanisms behind remodeling of the epigenetic landscape through nuclear mechanosensing, we utilize an innovative photostiffening hydrogel platform to manipulate nuclear mechanosensing in human mesenchymal stem cells. Our results reveal that disruption of nuclear mechanosensing up-regulates histone deacetylases and prevents epigenetic response as well as osteogenic fate determination. Interestingly, we see similar defective nuclear mechanosensing in bone from patients with osteoarthritis, indicating that this cellular mechanism is likely relevant to bone-related diseases.

Author contributions: A.R.K., C.J.W., and K.S.A. designed research; A.R.K. performed research; A.R.K. and K.S.A. analyzed data; and A.R.K., C.J.W., and K.S.A. wrote the paper.

Reviewers: C.A.G., Duke University; and K.A.K., University of New South Wales.

The authors declare no competing interest.

[1]To whom correspondence may be addressed. Email: Kristi.Anseth@colorado.edu.

This article contains supporting information online at https://www.pnas.org/lookup/suppl/doi:10.1073/pnas.2006765117/-/DCSupplemental.

First published August 17, 2020.

in situ stiffening, and the effect of nuclear tension on epigenetic remodeling can be studied as a function of time poststiffening. Furthermore, we use this material system to determine the sequence of cellular events taking place upon activation of nuclear mechanotransduction in a more precise manner.

Herein, we identify nuclear tension as a key mediator in epigenetic remodeling and osteogenic differentiation in hMSCs. First, in response to stiffening, we found that transmission of increased cytoskeletal tension to the nucleus, and thus the chromatin, increases histone acetylation and Runt-related transcription factor 2 (RUNX2) localization. Furthermore, increased nuclear tension decreases up-regulation and activity of type I HDACs. By inhibiting nuclear tension by disrupting the linker of nucleoskeleton and cytoskeleton (LINC) complex between the cytoskeleton and the nucleus through overexpression of a dominant negative (DN)-KASH, we observed a decrease in histone acetylation and osteogenesis. Therefore, we found that stiffness-mediated osteogenic differentiation is mediated through the LINC complex, resulting in an increase in nuclear tension, which subsequently directs epigenetic remodeling through down-regulation of HDACs. Inhibition of HDAC activity rescued histone acetylation and osteogenic fate determination in DN-KASH hMSCs during in situ stiffening. This finding is further supported by analysis of human osteoarthritic tissue by histological staining and qPCR. Defective nuclear mechanosensing is observed, as evidenced by down-regulated Lamin A/C messenger RNA (mRNA) expression. This corresponded to up-regulated HDAC mRNA expression and decreased histone acetylation, thereby suggesting reduced bone regenerative capacity.

As a summary, this work demonstrates the utility of dynamic hydrogels with phototunable mechanical properties to study the interplay of biophysical and biochemical signaling governing epigenetic remodeling and differentiation. Deciphering this language of forces and its effect on epigenetic remodeling of bone marrow-derived mesenchymal stem cells may shed light on potential targets for disease intervention.

Results

Nuclear Tension Increases over Time in hMSCs after In Situ Hydrogel Stiffening. To study the role of nuclear tension on epigenetic remodeling and fate determination in hMSCs, we utilize in situ stiffening PEG hydrogels prepared with azide/alkyne end-functionalized precursors as an hMSC culture platform. Using a stoichiometric excess of alkyne (DBCO) groups and following the spontaneous formation of the initial SPAAC gels, excess DBCO groups were cross-linked with a cytocompatible secondary photo-initiated reaction to stiffen the network in the presence of hMSCs (Fig. 1*A*). In these hydrogels, cell−matrix interactions were facilitated by the incorporation of 2 mM fibronectin mimetic RGD sequence (N_3-GRGDS). Hydrogels were generated in which Yes-associated protein (YAP), a well-studied protein that relays mechanical signals from the ECM to the nucleus (23), remains largely distributed in the cytoplasm (G' = 1 kPa). Exposure with 365-nm light for 2 min at 10 mW/cm^2 in the presence of 2 mM photoinitiator lithium phenyl-2,4,6-trimethylbenzoylphosphinate (LAP) generated stiff hydrogels designed to induce YAP nuclear translocation (24) (G' = 12 kPa) (Fig. 1 *B* and *C*). The hMSCs were cultured on soft hydrogels (G' = 1 kPa) for 24 h to allow adhesion. Subsequently, hMSC-laden hydrogels were exposed to light to stiffen the gel (G' = 12 kPa), and the hMSC response was analyzed at 0, 1, 3, 24, 72, and 120 h after in situ stiffening (Fig. 1*D*). As expected, YAP translocated from the cytoplasm to the nucleus within 24 h to 72 h post in situ stiffening, shown by the increase in the YAP nuclear/cytoplasm (nuc/cyt) ratio from ∼1.2 to ∼1.8 (*SI Appendix*, Fig. S1). To control for time-dependent changes, the 120-h time point after in situ stiffening was compared to a soft hydrogel that did not undergo stiffening (*SI Appendix*, Fig. S2). These results illustrate that hMSCs are responsive to the dynamic changes in the shear elastic modulus of the SPAAC hydrogels.

Next, to understand whether in situ stiffening leads to increased nuclear tension, we analyzed cell and nucleus area, as they have been implicated as potential markers of cellular tension (25). The cytoplasm area was significantly larger after 24 h poststiffening, but F-actin stress fibers were observed only after 72 h. The nuclear area was significantly increased from ∼150 μm^2 to ∼225 μm^2 after 72 h, correlating with the time frame of F-actin stress fiber formation (Fig. 1 *E*–*G*). These results potentially suggest that changes in cytoplasmic morphology precede increased cytoskeletal tension via stress fiber formation, as well as changes in nuclear morphology. To understand how cytoskeletal tension could be transmitted to the nucleus, we next looked at Lamin A levels, as Lamin A has been known to play a key role in force transmission through cytoplasm to the nucleus via the LINC complex (7, 26). We characterized Lamin A intensity over time after stiffening. A significant increase was seen after 72 h poststiffening, again correlating with observed F-actin fibers and increased nuclear area (Fig. 1*H*). This increase in Lamin A intensity was confirmed by Lamin A protein expression and mRNA expression analysis, for which a twofold increase was observed (Fig. 1 *I* and *J* and *SI Appendix*, Fig. S3). To control for time-dependent changes, the 120-h time point after in situ stiffening was compared to a soft hydrogel that did not undergo stiffening (*SI Appendix*, Fig. S2). We conclude that photostiffening PEG hydrogels can be used to induce nuclear tension in hMSCs and initiate nuclear mechanosensing. Therefore, the model system was next used to study the influence of nuclear mechanosensing on epigenetic remodeling and osteogenic fate commitment.

Epigenetic Remodeling and Osteogenic Commitment Induced by Increase in Nuclear Tension. Besides the cytoskeleton being linked to Lamin A through the LINC complex, Lamin A is also anchored to chromatin. Therefore, cytoskeletal tension has the potential to directly alter chromatin localization and gene expression (27). With this in mind, we next assessed whether stretching of the nuclear membrane can mechanically perturb the chromatin and change epigenetic remodeling, and, if so, on what time scale these events will take place. We analyzed global histone acetylation as a marker for chromatin remodeling between 0 h and 120 h after in situ stiffening and found it to significantly increase by 1.5-fold at 72 h poststiffening (Fig. 2 *A* and *B* and *SI Appendix*, Fig. S2). This increase was confirmed by analyzing histone 3 acetylation protein levels via Western blotting. (Fig. 2*C* and *SI Appendix*, Fig. S3).

Next, we examined the effect of substrate stiffening on osteogenic fate commitment. The RUNX2 nuc/cyt ratio was analyzed as a marker for osteogenic activation and quantified at all time points after stiffening. Again, a significant increase in RUNX2 nuclear localization was observed at 72 h poststiffening (Fig. 2 *A* and *D*). The immunostaining analysis was further confirmed by RUNX2, PPARγ, and CD105 mRNA analysis. Indeed, RUNX2 mRNA expression was threefold increased at 72 h compared to 0 h, while PPARγ, an adipogenic transcription factor, and CD105, a multipotency marker, mRNA expression remained constant, suggesting osteogenic fate commitment at 72 h. Both histone acetylation and RUNX2 levels were at its highest at 72 h poststiffening, correlating with the time frame in which nuclear tension in the cultured hMSCs was established (Fig. 1), indicating that nuclear tension might be necessary to induce histone acetylation and RUNX2 nuclear localization.

Disruption of Nuclear Mechanosensing Up-Regulates HDACs and Prevents Epigenetic Response and Fate Determination. Our results suggest that nuclear tension controls histone acetylation and RUNX2 localization, but, to validate its specific role in chromatin remodeling and fate determination, we next altered nuclear mechanosensing by disrupting the LINC complex. This disruption was achieved by uncoupling the cytoskeleton from the nuclear lamina by stably introducing a dominant negative nesprin

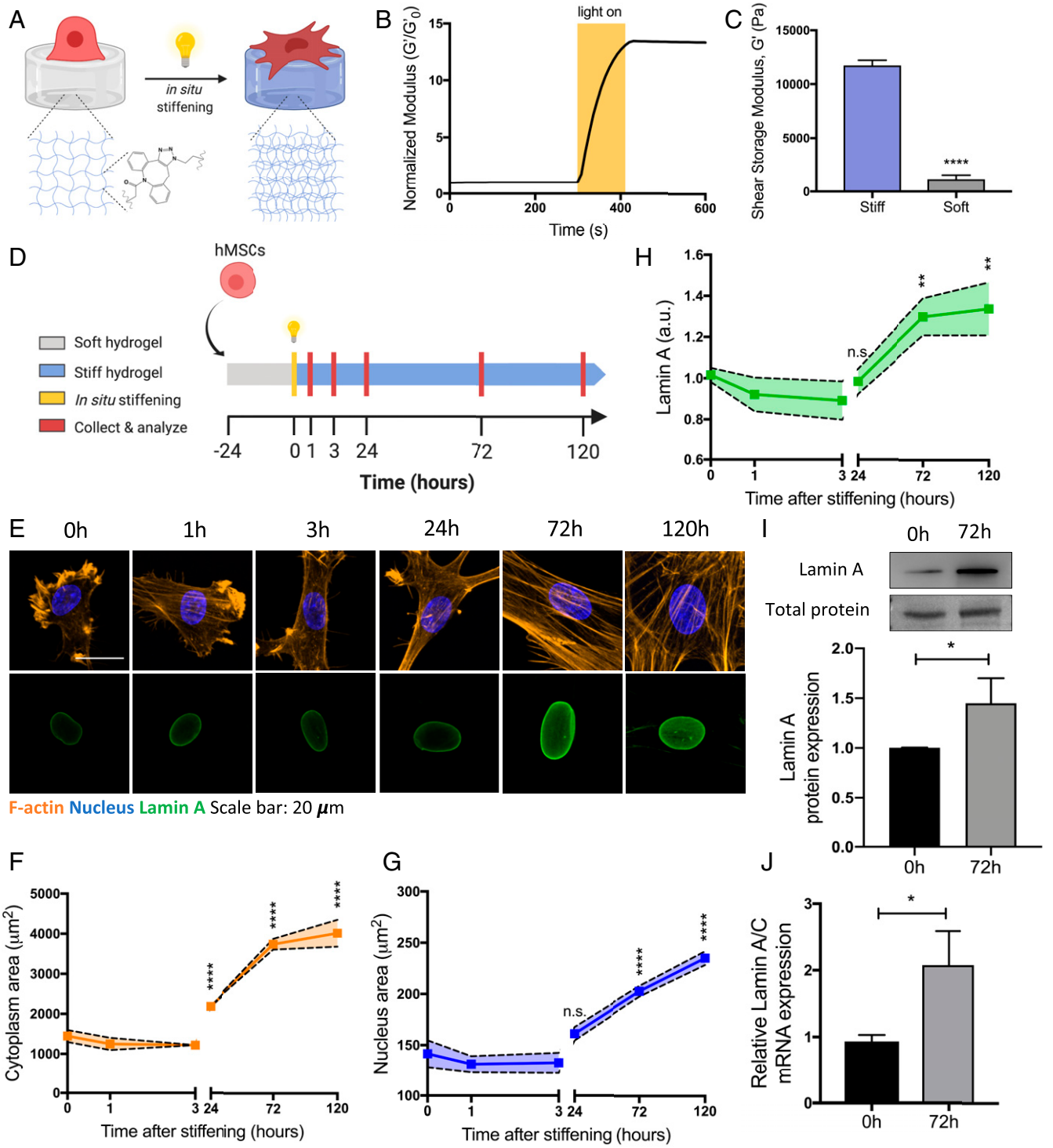

Fig. 1. In situ stiffening hydrogel culture system induces nuclear tension in hMSCs. (*A*) Schematic illustration of the SPAAC hydrogel synthesis, which can be stiffened in the presence of the cells upon a secondary photo-cross-linking reaction in the presence of excess DBCO groups. (*B*) SPAAC reaction occurs spontaneously upon mixing azide and DBCO-functionalized multiarm PEG precursors to form a G′ = 1 kPa initial network. Subsequent light illumination (10 mW/cm^2, 365 nm, 120 s) in the presence of a photoinitiator (LAP, 2 mM) cross-links the excess DBCO groups, resulting in a final modulus of G′ = 12 kPa. (*C*) Shear storage modulus of soft hydrogel condition (G′ = 1 kPa) and stiff hydrogel condition (G′ = 12 kPa). Student's *t* test applied, $n = 3$ gels. (*D*) Experimental design in which hMSCs were cultured on soft hydrogels (gray) for 24 h, which were then further cross-linked with light (yellow) to yield stiff hydrogels (blue). The hMSCs were cultured for 1, 3, 24, 72, or 120 h poststiffening, collected, and analyzed (red). (*E*) Representative images of hMSCs cultured on hydrogels for varying times. DAPI, blue; F-actin, yellow; Lamin A, green. (Scale bar: 20 μm.) (*F–H*). Quantification of hMSC nuclear and cytoplasmic areas and Lamin A intensity of hMSCs at 0 h and between 0 h and 120 h poststiffening. Compared to t = 0 with one-way ANOVA test with Dunnett's post hoc applied, $n > 3$ gels. (*I*) Western blot and quantification of Lamin A/C protein expression for t = 0 h and t = 72 h Student's *t* test applied, $n = 3$ gels. (*J*) Quantification of Lamin A/C mRNA expression for t = 0 h and t = 72 h Student's *t* test applied, $n = 3$ gels with triplicates; n.s., not significant; *: $P < 0.05$; **: $P < 0.01$; ****: $P < 0.0001$. The data represent the mean value ± SD.

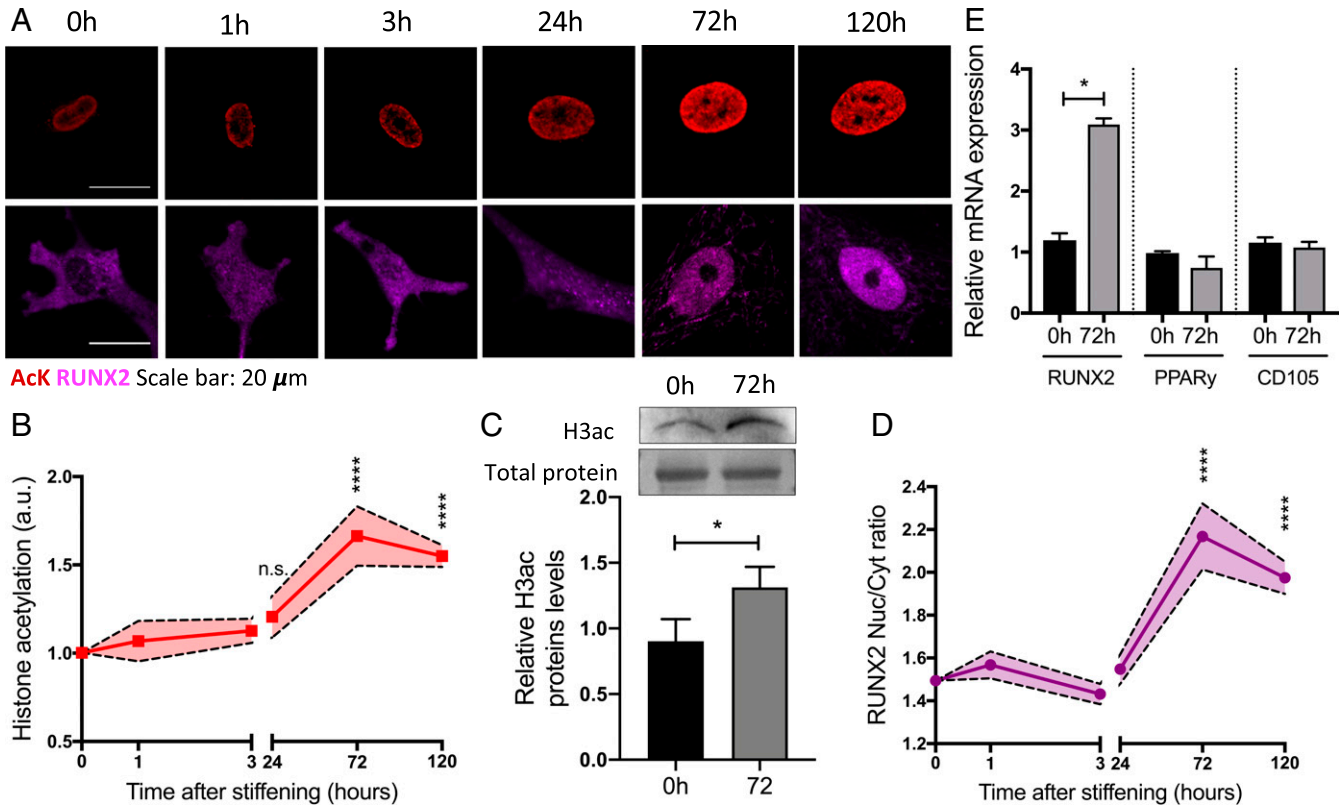

Fig. 2. Nuclear tension increases histone acetylation and RUNX2 in hMSCs. (*A*) Representative images of hMSCs cultured on hydrogels between 0 h and 120 h poststiffening. Histone acetylation, red; RUNX2, purple. (Scale bar: 20 μm.) (*B*) Quantification of histone acetylation in hMSCs between 0 h and 120 h poststiffening. Compared to t = 0 h with one-way ANOVA with Dunnett's post hoc applied, $n = 3$ gels. (*C*) Western blot and quantification of histone acetylation protein expression for t = 0 h and t = 72 h Student's *t* test applied, $n = 3$ gels. (*D*) Quantification of RUNX2 nuc/cyt ratio in hMSCs at 0 h and over time after stiffening. Compared to t = 0 h with one-way ANOVA with Dunnett's post hoc applied, $n = 3$ gels. (*E*) Quantification of mRNA expression of RUNX2, PPARy, and CD105 at t = 0 h and t = 72 h Student's *t* test applied, $n = 3$ gels with triplicates. *: $P < 0.05$; ****: $P < 0.0001$. The data represent the mean value ± SD.

construct containing the C-terminal KASH domain fused to an N-terminal mCherry (28). Overexpression of the DN-KASH domain allows for precise binding to endogenous SUN proteins at the nuclear envelope, thereby displacing endogenous nesprins from the nuclear envelope (28) (Fig. 3*A*). To determine whether stable introduction of DN-KASH disrupts nuclear mechanosensing, hMSCs overexpressing DN-KASH, as well as control cells that only express the mCherry construct, were seeded on in situ stiffening hydrogels and monitored between 0 h and 120 h poststiffening (Fig. 3*B*). The nuclear area of DN-KASH hMSCs showed no increase after stiffening, with no significant change from 0 h, but with significant differences from the mCherry control at 72 and 120 h (*SI Appendix*, Fig. S4*A*). Interestingly, overexpression of DN-KASH also decreased the cytoplasm area of the hMSCs after stiffening. Cytoplasm area showed a slight increase over time, but was not significantly different from 0 h, and was statistically different from the mCherry control (*SI Appendix*, Fig. S4*B*). However, immunostaining images showed F-actin fiber formation (*SI Appendix*, Fig. S4*C*). In addition, Lamin A/C mRNA expression showed no increase after stiffening at 72 h compared to 0 h in the DN-KASH hMSCs, in contrast to the mCherry hMSCs (*SI Appendix*, Fig. S4*D*). Together, these results demonstrate that overexpression of DN-KASH disrupts nuclear mechanosensing.

Next, we sought to test whether chromatin remodeling and osteogenic fate commitment were altered in the DN-KASH hMSCs. Histone acetylation did not increase after stiffening and was ∼50% lower at 72 h after stiffening compared to mCherry control (Fig. 3 *C* and *D* and *SI Appendix*, Fig. S5). The same trend was observed for RUNX2 localization. While RUNX2 was primarily located in the nucleus at 72 h (nuc/cyt ratio of ∼2) after stiffening for the mCherry controls, RUNX2 remained more cytoplasmic (nuc/cyt ratio of ∼1.5) for the DN-KASH–overexpressing hMSCs (Fig. 3 *C* and *E*). Likewise, the YAP nuc/cyt ratio showed similar trends, as it has been shown to correlate with osteogenic commitment as well (*SI Appendix*, Fig. S6). RUNX2 immunostaining trends were confirmed by RUNX2 mRNA analysis (Fig. 3*F*). While RUNX2 mRNA expression remained low over time after stiffening, PPARy localization and mRNA expression showed the opposite trend, where they increased in DN-KASH hMSCs (*SI Appendix*, Fig. S7). These results suggest that these "uncoupled" hMSCs have a desensitized mechanotransduction and sense their environment as if they remained on soft hydrogels even after the stiffening event.

After verifying that nuclear mechanotransduction mediated epigenetic remodeling and osteogenic commitment, we delved deeper into the mechanism of this signal transduction. Chromatin condensation and histone acetylation are regulated by epigenetic modulators, such as type I HDACs. HDAC1, HDAC2, and HDAC3 have been implicated in playing a role in osteogenic differentiation of hMSCs (20, 29–31). To investigate whether disruption of the KASH domain leads to altered activity and levels of HDAC enzymes, we analyzed mRNA expression of HDAC1, HDAC2, and HDAC3. Interestingly, we found that all three HDACs were highly upregulated at 0 and 72 h after stiffening in DN-KASH hMSCs, while, for the mCherry controls, HDAC expression decreased after substrate stiffening (Fig. 3*G*). We verified that HDAC expression correlates with HDAC activity by performing an in situ

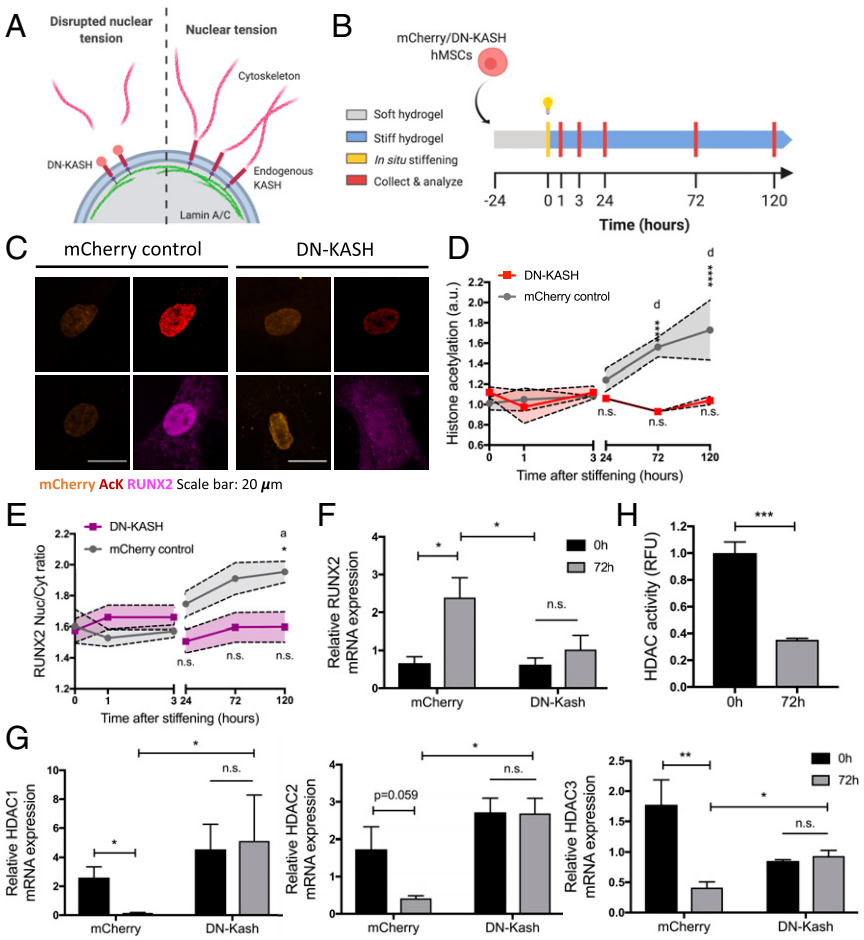

Fig. 3. Disruption of nuclear tension prevents epigenetic response and fate determination via HDAC up-regulation. (*A*) Schematic showing the mechanism of DN-KASH overexpression resulting in disrupted nuclear tension. (*B*) Experimental design in which mCherry or DN-KASH hMSCs were cultured on soft hydrogels (gray) for 24 h. Subsequently, hydrogels were in situ stiffened (yellow) to stiff hydrogels (blue), and hMSCs were cultured for another 1, 3, 24, 72, or 120 h before collection and analysis (red). (*C*) Representative images of mCherry and DN-KASH hMSCs cultured on hydrogels at t = 72 h; mCherry, orange; histone acetylation, red; RUNX2, purple. (Scale bar: 20 μm.) (*D* and *E*) Quantification of histone acetylation and RUNX2 nuc/cyt ratio in mCherry and DN-KASH hMSCs between 0 h and 120 h poststiffening. Results are compared to t = 0 h with one-way ANOVA with Dunnett's post hoc applied; mCherry is compared to DN-KASH with one-way ANOVA with Sidak post hoc applied; $n > 3$ gels. (*F*) Quantification of RUNX2 mRNA expression for mCherry and DN-KASH hMSCs at t = 0 h and t = 72 h. One-way ANOVA with Tukey post hoc applied, $n = 3$ gels with triplicates. (*G*) Quantification of HDAC1, HDAC2, and HDAC3 mRNA expression for mCherry and DN-KASH hMSCs at t = 0 h and t = 72 h. One-way ANOVA with Tukey post hoc applied, $n = 3$ gels with triplicates. (*H*) Quantification of HDAC activity for hMSCs at t = 0 h and t = 72 h. Student's *t* test applied, $n = 4$. * or a: $P < 0.05$; **: $P < 0.01$; ***: $P < 0.001$; **** or d: $P < 0.0001$. The data represent the mean value ± SD.

HDAC activity assay and observed a threefold decrease in activity at 72 h poststiffening (Fig. 3*H*). Together, these results suggest nuclear tension is necessary to decrease HDAC activity, which, in turn, increases histone acetylation and RUNX2 expression as well as its nuclear localization to direct hMSCs into an osteogenic phenotype.

HDAC Inhibition Rescues Epigenetic Remodeling and Fate Determination. Impaired nuclear mechanotransduction, by decoupling the cytoskeleton from the nuclear envelope, resulted in increased HDAC expression and activity, leading to lower RUNX2 nuclear localization. With this in mind, we explored whether the histone acetylation levels and RUNX2 nuclear localization could be rescued by blocking HDAC activity with Trichostatin A (TSA), a known HDAC inhibitor (32). First, we verified the inhibitory effect of TSA on HDAC activity by carrying out an in situ HDAC activity assay in hMSCs cultured on stiffening hydrogels for 72 h (Fig. 4*A*). Next, we sought to determine whether TSA can revert the defective nuclear mechanosensing in DN-KASH transduced hMSCs. For these experiments, hMSCs were first cultured on soft hydrogels for 24 h, and treated with TSA (300 nM) at the onset of in situ stiffening, and histone acetylation, nuclear area, and RUNX2 nuc/cyt ratio were analyzed between 0 h and 120 h poststiffening (Fig. 4*B*). TSA treatment completely rescued histone acetylation after substrate stiffening in DN-KASH transduced hMSCs within 120 h, as histone acetylation levels reached that of mCherry expression control cells (Fig. 4 *C* and *D* and *SI Appendix*, Fig. S8). Similarly, complete rescue of the nuclear area and RUNX2 nuc/cyt ratio was also observed upon TSA treatment (Fig. 4 *C*, *E*, and *F* and *SI Appendix*, Fig. S8), indicating that inhibition of HDACs increases not only histone acetylation but also chromatin accessibility. These results indicate that HDAC inhibition in hMSCs with a dysregulated nuclear mechanosensing rescues their osteogenic potential.

Dysregulation of Nuclear Mechanosensing Observed in Osteoarthritis. Dysregulation of nuclear mechanosensing has been recently implicated in bone-specific defects, such as osteoporosis and osteoarthritis, as well as metastases to bone (15–17); however, it is unclear how disruption of nuclear mechanosensing may exacerbate these

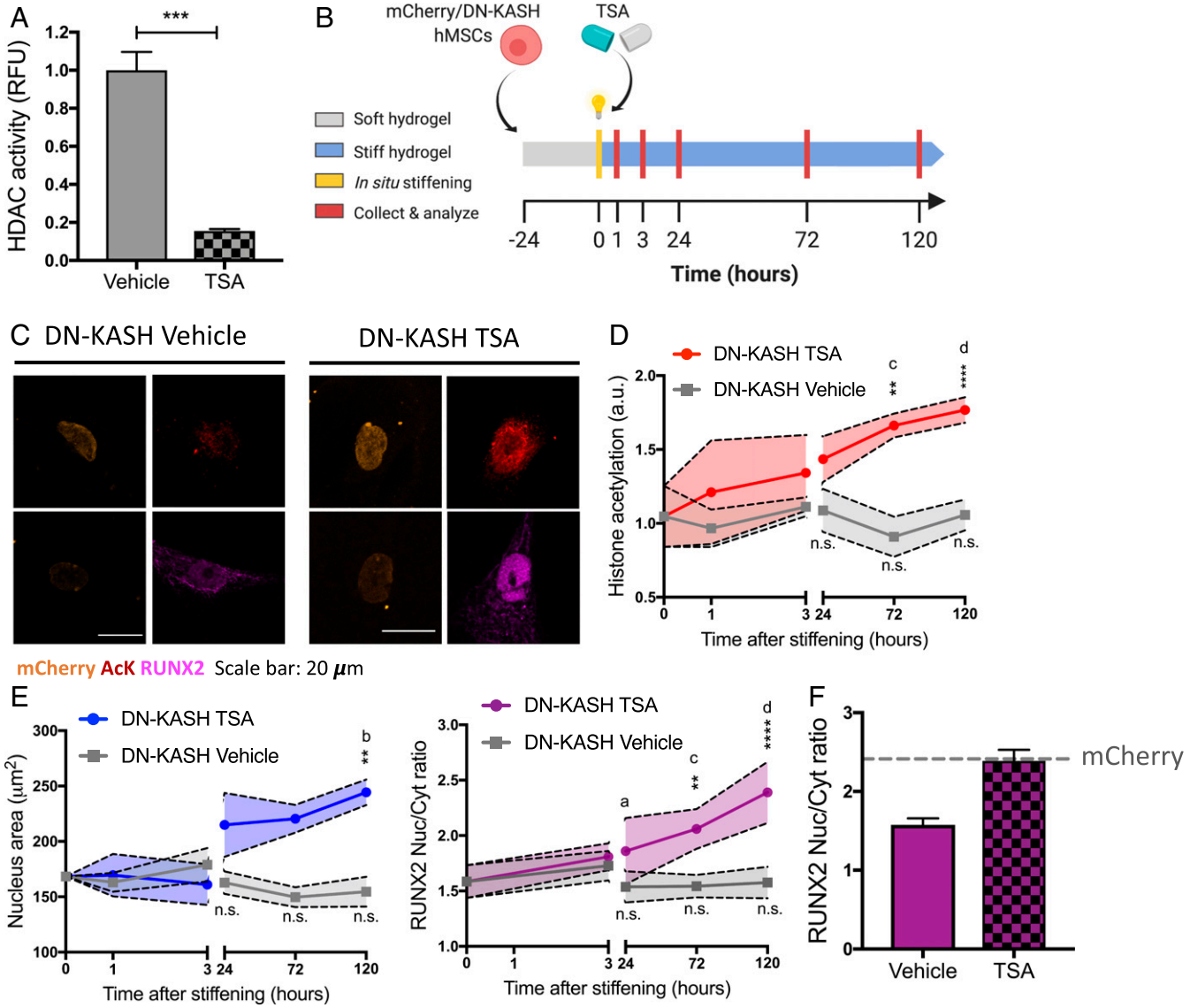

Fig. 4. Dysregulation of epigenetic response and fate determination can be rescued via HDAC inhibition. (*A*) Quantification of HDAC activity for hMSCs with and without TSA treatment. Student's *t* test applied, $n = 4$ gels. (*B*) Experimental design in which mCherry or DN-KASH hMSCs were cultured on soft hydrogels (gray) for 24 h. Subsequently, hydrogels were in situ stiffened (yellow) to stiff hydrogels (blue), and TSA or vehicle was added to the culture. The hMSCs were cultured for another 1, 3, 24, 72, or 120 h before they were collected and analyzed (red). (*C*) Representative images of mCherry and DN-KASH hMSCs cultured on hydrogels at t = 72 h with and without TSA treatment; mCherry, orange; histone acetylation, red; RUNX2, purple. (Scale bar: 20 μm.) (*D*) Quantification of histone acetylation in DN-KASH hMSCs with and without TSA treatment between 0 h and 120 h poststiffening. Results are compared to t = 0 h with one-way ANOVA with Dunnett's post hoc applied. DN-KASH vehicle is compared to DN-KASH TSA with one-way ANOVA with Sidak post hoc applied, $n > 3$ gels. (*E*) Quantification of nuclear area and RUNX2 nuc/cyt ratio in DN-KASH hMSCs with and without TSA treatment between 0 ha and 120 h poststiffening. Results are compared to t = 0 h with one-way ANOVA with Dunnett's post hoc applied. DN-KASH vehicle is compared to DN-KASH TSA with one-way ANOVA with Sidak post hoc applied, $n > 3$ gels. (*F*) Quantification of RUNX2 nuc/cyt ratio in DN-KASH hMSCs with and without TSA treatment at 120 h, compared to mCherry TSA treatment (dotted control line). a: $P < 0.05$; ** or b: $P < 0.01$; *** or c: $P < 0.001$; **** or d: $P < 0.0001$. The data represent the mean value ± SD.

bone-specific diseases. Therefore, we sought to understand whether cells residing in osteoarthritic tissue may have dysregulated nuclear tension, and, as a result, have decreased histone acetylation and increased HDAC expression in osteoarthritic tissue. To study this, histone acetylation intensity per nucleus was analyzed in human subchondral bone tissue isolated from a patient diagnosed with osteoarthritis. Histone acetylation levels are significantly lower in cells in the diseased tissue compared to healthy bone tissue (Fig. 5 *A* and *B* and *SI Appendix*, Fig. S9). Analyzing the tissue for Lamin A/C expression confirmed that osteoarthritic bone had ∼80% lower Lamin A/C mRNA expression compared to healthy bone tissue, suggesting that defective nuclear mechanosensing may be responsible for reduced chromatin accessibility (Fig. 5*C*). Furthermore, HDAC1, HDAC2, and HDAC3 expression was highly up-regulated in the osteoarthritic bone compared to healthy bone (Fig. 5*D*). These results suggest that, in osteoarthritis, nuclear mechanosensing might be impaired with lower Lamin A/C expression, thereby up-regulating HDACs, resulting in lower bone regenerative potential. The osteoarthritic cells mechanoresponsiveness resembles aspects of that of the DN-KASH-expressing hMSCs, in which the mechanotransduction machinery has been desensitized and more closely resembles cells cultured on soft gels.

Discussion

Bone degenerative diseases are a major medical problem in the elderly population and can lead to increased disability and

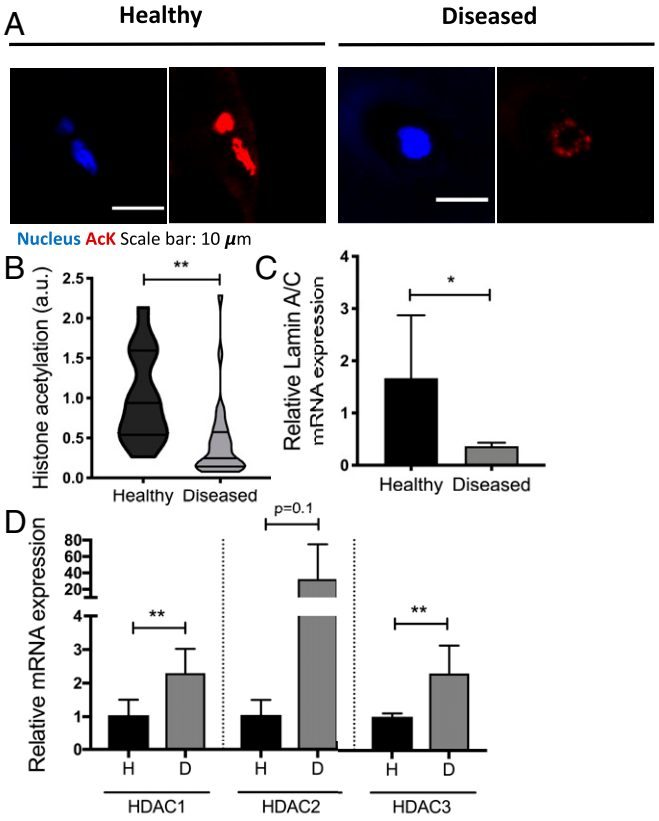

Fig. 5. Misregulation of nuclear sensing and up-regulation of HDACs in osteoarthritis. (*A*) Representative images of histone acetylation staining from healthy or diseased male human bone tissue. Histone acetylation, red; DAPI, blue. (Scale bar: 10 μm.) (*B*) Quantification of histone acetylation in healthy and diseased tissue. Student's *t* test applied, $n > 15$ cells. Values are shown as median ± 1.5 interquartile range. (*C*) Quantification of Lamin A/C mRNA expression from healthy or diseased female human bone tissue. Student's *t* test applied, $n = 2$ donors. (*D*) Quantification of HDAC1, HDAC2, and HDAC3 mRNA expression from healthy or diseased female human bone tissue. Student's *t* test applied, $n = 2$ donors. *: $P < 0.05$; **: $P < 0.01$. The data represent the mean value ± SD.

mortality (33). Dysregulated hMSCs are one of the key cellular mediators of bone degeneration, and, here, we aimed to understand whether alterations in nuclear mechanosensing and the mechanisms responsible contribute to MSC dysregulation. As part of our in-depth study, we used hydrogel materials with dynamically adjustable moduli to elucidate mechanosensing pathways that might block or promote bone regeneration. We demonstrated that stiffness-mediated osteogenic fate commitment is driven by epigenetic remodeling through nuclear mechanosensing (Fig. 2). We show that disruption of nuclear mechanosensing abolishes this response by up-regulating HDAC expression and increasing its activity (Fig. 3). Furthermore, we show that pharmacological inhibition of HDAC activity rescues the epigenetic and osteogenic response in hMSCs with pathological nuclear mechanosensing (Fig. 4). These in vitro results show striking correlations with our findings in human osteoarthritic subchondral bone tissue (Fig. 5). Defective nuclear mechanosensing was evidenced by down-regulation of Lamin A/C mRNA expression and corresponded to up-regulated HDAC mRNA expression and lower histone acetylation, thereby suggesting reduced bone regenerative capacity.

The cytoskeleton, LINC complex, and the physical attachment to nuclear lamins have been shown to be highly important in nuclear integrity, chromatin remodeling, and subsequent differentiation or cell reprogramming (34, 35). Multiple mechanisms have been suggested for Lamin A/C contribution to transcriptional changes. One mechanism involves direct force propagation from the actin cytoskeleton through the LINC complex to the nucleus, which physically stretches the chromatin and thereby up-regulates transcription (27). Alternatively, it has been hypothesized that nuclear tension can deform the lamina, enabling the release or sequestration of transcription factors or epigenetic modifiers (26, 36–38). In our study, we revealed a significant decrease in HDAC activity with an increase in Lamin A/C expression when hMSCs were cultured on stiff hydrogel microenvironments (i.e., 72 h after in situ stiffening). The latter mechanism could support our findings that stiffness-induced nuclear tension by up-regulation of Lamin A/C might be involved in lamina–HDAC interactions, thereby inactivating HDACs and altering transcription. We have seen drastic HDAC1 and HDAC3 down-regulation after hydrogel stiffening in hMSCs (Fig. 3), which follows trends of previously published work in which HDAC1 decreases during osteogenic differentiation, and acetylation of histone 3 and 4 increases at the promoter of osteocalcin, an indicator of active gene transcription (29, 39). In addition, it has been shown that HDAC3 can physically interact with the RUNX2 promoter, thereby deacetylating histone 3 and suppressing the transcription activity of RUNX2 (29). Remarkably, disrupting nuclear mechanosensing inhibited a stiffness-induced up-regulation of Lamin A/C, which correlated to an increase in HDAC expression. Together, this supports the idea that there is an interplay of physical and protein signaling that governs the transcriptional changes seen here in hMSCs over time after substrate stiffening. Ultimately, analyzing the location of these changes in global levels of histone acetylation or characterizing more specific histone acetylation modification (e.g., H3K9ac) within the nucleus could shed light on the earlier changes happening after substrate stiffening and may disentangle the interplay of physical and protein signaling.

Beyond these in vitro studies and results, aberrant mechanotransduction has also been implicated in bone degenerative diseases. Researchers have observed a decrease in Lamin A/C expression with age and its negative effect on bone formation (16, 40). Furthermore, changes in the epigenetic landscape have been characterized, such as up-regulation of microRNAs (miRNAs), that target silencing of osteogenic miRNAs in osteoporotic serum (41), deletion of miRNAs that cause osteoarthritis (42), and differentially methylated genes, including RUNX2 in osteoarthritic patients (43, 44). Our results (Fig. 5) now link disrupted nuclear mechanosensing with a decrease in Lamin A/C expression to aberrant epigenetic remodeling in osteoarthritic bone tissue. This aberrant remodeling results in increased HDAC expression, suggesting that this might lead to lower RUNX2 expression and thereby decreased bone formation.

Age-related bone loss is not only associated with low levels of osteoblast differentiation but also with higher levels of adipocyte differentiation. However, the mechanism behind this change in balance remains unclear (45). We show that overexpressing DN-KASH in hMSCs resulted in desensitized hMSCs that could not respond to increases in the mechanics of their microenvironment. Instead, results reveal that these hMSCs behave as if they remain in their initially soft microenvironment, even after in situ stiffening of the hydrogel, and express low levels of RUNX2 (Fig. 3*F*), but increase the expression of PPARγ (*SI Appendix*, Fig. S7). This mechanical desensitization has also been seen in MSCs from older donors, where YAP nuclear translocation is decreased and RUNX2 expression is down-regulated on stiff gels compared to young MSCs (46, 47). Even with passaging, this dysregulation has been observed (6). Furthermore, the blocked nuclear mechanosensing might have induced a feedback loop to the cytoplasm; a possible reason why we observed a decrease in cell spreading with stiffening compared to the mCherry control (*SI Appendix*, Fig. S4). This result suggests that not only nuclear

mechanosensing, but also complete disruption of the cellular mechanosensing, leads to the observed adipogenic cell response. Mechanical desensitization might develop with aging, which could potentially bias hMSCs toward adipogenic differentiation, contributing to well-known imbalances in the differentiation in osteoporosis and other porous bone diseases.

Novel biomaterial chemistries are enabling innovative experiments to be performed to test hypotheses related to in vivo findings and improve the field's understanding of mechanotransduction as it relates to disease, aging, and wound healing. Here, we used a phototunable hydrogel system to induce nuclear tension and study its effects on epigenetic remodeling and fate commitment. The precise and cytocompatible conditions of the in situ stiffening reaction enabled us to study the time dynamics of cytoplasmic and nuclear tension, chromatin remodeling, and fate commitment at short time periods after the stiffening event (Figs. 1 and 2). This hydrogel and related material systems (48–52) are highly advantageous for studying mechanotransduction events that rapidly reach a steady state, such as calcium signaling, when cultured on materials with static properties. However, these events can be directly observed in real time when using biomaterials systems with properties that can be changed on demand.

Our experiments provide insight into pathways that contribute to stiffness-induced osteogenic fate commitment through epigenetic remodeling and show that these in vitro results can inform about in vivo diseases such as osteoarthritis. As the field progresses, this understanding should assist in the identification of potential therapeutic targets for disease intervention. Literature suggests that inhibitors of class I, II, and IV HDACs could increase the lifespan of people, as several age-related preclinical disease models, ranging from neurodegeneration to heart disease, show improvement upon HDAC inhibition (53, 54). For mediate bone degeneration, TSA has been shown to inhibit osteoclast differentiation, resulting in decreased bone resorption (55). Here we show that inhibition of HDAC1 or HDAC3 could have beneficial effects on the differentiation of hMSCs into osteoblasts to subsequently increase bone density for patients with bone degeneration, such as osteoarthritis or osteoporosis. Besides HDACs as drug targets, stabilization of the F-actin cytoskeleton and increasing the nuclear tension could also help rescue osteogenic differentiation. Finally, our findings can provide knowledge for the maintenance of multipotency during expansion of hMSCs for clinical therapies.

Taken together, our findings highlight a mechanism by which nuclear tension inhibits HDACs and promotes histone acetylation leading to osteogenic fate determination, potentially explaining phenotypes seen in bone degenerative diseases and laminopathies.

Materials and Methods

The hMSCs were isolated from fresh human bone marrow (Lonza). P2 hMSCs were cultured on phototunable hydrogels, and, subsequently, hydrogels were in situ stiffened using 365-nm light. Cell morphology and protein abundance were analyzed similarly to previous studies (19). For complete details on methods, please refer to *SI Appendix*.

Data Availability. All study data are included in the article and *SI Appendix*.

ACKNOWLEDGMENTS. We acknowledge the support of the NIH (Grants R01 RHL132353-01 and R21 AR067469). A.R.K. was supported by Department of Education Graduate Assistance in Areas of National Need (DoE GAANN) fellowship. C.J.W. was supported by NSF Training Grant IGERT 1144807, NIH Predoctoral Fellowship F31HL142223, and DoE GAANN Biomaterials Fellowship. Kemal Arda Günay is thanked for helpful discussions and for manuscript preparation. Figure schematics were created with BioRender.com.

1. W. P. Daley, S. B. Peters, M. Larsen, Extracellular matrix dynamics in development and regenerative medicine. *J. Cell Sci.* **121**, 255–264 (2008).
2. F. Guilak *et al.*, Control of stem cell fate by physical interactions with the extracellular matrix. *Cell Stem Cell* **5**, 17–26 (2009).
3. G. Nardone *et al.*, YAP regulates cell mechanics by controlling focal adhesion assembly. *Nat. Commun.* **8**, 15321 (2017).
4. A. W. Orr, B. P. Helmke, B. R. Blackman, M. A. Schwartz, Mechanisms of mechanotransduction. *Dev. Cell* **10**, 11–20 (2006).
5. C. Yang *et al.*, Spatially patterned matrix elasticity directs stem cell fate. *Proc. Natl. Acad. Sci. U.S.A.* **113**, E4439–E4445 (2016).
6. V. V. Rao, M. K. Vu, H. Ma, A. R. Killaars, K. S. Anseth, Rescuing mesenchymal stem cell regenerative properties on hydrogel substrates post serial expansion. *Bioeng. Transl. Med.* **4**, 51–60 (2018).
7. T. Bouzid *et al.*, The LINC complex, mechanotransduction, and mesenchymal stem cell function and fate. *J. Biol. Eng.* **13**, 68 (2019).
8. C. Uhler, G. V. Shivashankar, Regulation of genome organization and gene expression by nuclear mechanotransduction. *Nat. Rev. Mol. Cell Biol.* **18**, 717–727 (2017).
9. K. N. Dahl, A. J. S. Ribeiro, J. Lammerding, Nuclear shape, mechanics, and mechanotransduction. *Circ. Res.* **102**, 1307–1318 (2008).
10. S.-J. Heo *et al.*, Mechanically induced chromatin condensation requires cellular contractility in mesenchymal stem cells. *Biophys. J.* **111**, 864–874 (2016).
11. N. Jain, K. V. Iyer, A. Kumar, G. V. Shivashankar, Cell geometric constraints induce modular gene-expression patterns via redistribution of HDAC3 regulated by actomyosin contractility. *Proc. Natl. Acad. Sci. U.S.A.* **110**, 11349–11354 (2013).
12. M. Rabineau *et al.*, Chromatin de-condensation by switching substrate elasticity. *Sci. Rep.* **8**, 12655 (2018).
13. D. E. Jaalouk, J. Lammerding, Mechanotransduction gone awry. *Nat. Rev. Mol. Cell Biol.* **10**, 63–73 (2009).
14. C. M. Gordon *et al.*, Hutchinson-Gilford progeria is a skeletal dysplasia. *J. Bone Miner. Res.* **26**, 1670–1679 (2011).
15. C. Ghayor, F. E. Weber, Epigenetic regulation of bone remodeling and its impacts in osteoporosis. *Int. J. Mol. Sci.* **17**, 1446 (2016).
16. G. Duque, D. Rivas, Age-related changes in lamin A/C expression in the osteoarticular system: Laminopathies as a potential new aging mechanism. *Mech. Ageing Dev.* **127**, 378–383 (2006).
17. D. E. Ingber, Mechanobiology and diseases of mechanotransduction. *Ann. Med.* **35**, 564–577 (2003).
18. F. M. Pérez-Campo, J. A. Riancho, Epigenetic mechanisms regulating mesenchymal stem cell differentiation. *Curr. Genomics* **16**, 368–383 (2015).
19. A. R. Killaars *et al.*, Extended exposure to stiff microenvironments leads to persistent chromatin remodeling in human mesenchymal stem cells. *Adv. Sci. (Weinh.)* **6**, 1801483 (2018).
20. K. H. Park-Min, Epigenetic regulation of bone cells. *Connect. Tissue Res.* **58**, 76–89 (2017).
21. C. A. DeForest, B. D. Polizzotti, K. S. Anseth, Sequential click reactions for synthesizing and patterning three-dimensional cell microenvironments. *Nat. Mater.* **8**, 659–664 (2009).
22. T. E. Brown *et al.*, Secondary photocrosslinking of click hydrogels to probe myoblast mechanotransduction in three dimensions. *J. Am. Chem. Soc.* **140**, 11585–11588 (2018).
23. S. Dupont *et al.*, Role of YAP/TAZ in mechanotransduction. *Nature* **474**, 179–183 (2011).
24. A. J. Engler, S. Sen, H. L. Sweeney, D. E. Discher, Matrix elasticity directs stem cell lineage specification. *Cell* **126**, 677–689 (2006).
25. S. B. Khatau *et al.*, A perinuclear actin cap regulates nuclear shape. *Proc. Natl. Acad. Sci. U.S.A.* **106**, 19017–19022 (2009).
26. J. Swift *et al.*, Nuclear lamin-A scales with tissue stiffness and enhances matrix-directed differentiation. *Science* **341**, 1240104 (2013).
27. T. Dechat *et al.*, Nuclear lamins: Major factors in the structural organization and function of the nucleus and chromatin. *Genes Dev.* **22**, 832–853 (2008).
28. M. L. Lombardi *et al.*, The interaction between nesprins and sun proteins at the nuclear envelope is critical for force transmission between the nucleus and cytoskeleton. *J. Biol. Chem.* **286**, 26743–26753 (2011).
29. H. W. Lee *et al.*, Histone deacetylase 1-mediated histone modification regulates osteoblast differentiation. *Mol. Endocrinol.* **20**, 2432–2443 (2006).
30. Y. Fu *et al.*, Histone deacetylase 8 suppresses osteogenic differentiation of bone marrow stromal cells by inhibiting histone H3K9 acetylation and RUNX2 activity. *Int. J. Biochem. Cell Biol.* **54**, 68–77 (2014).
31. T. L. Downing *et al.*, Biophysical regulation of epigenetic state and cell reprogramming. *Nat. Mater.* **12**, 1154–1162 (2013).
32. H. H. Cho *et al.*, Induction of osteogenic differentiation of human mesenchymal stem cells by histone deacetylase inhibitors. *J. Cell. Biochem.* **96**, 533–542 (2005).
33. J. R. Curtis, M. M. Safford, Management of osteoporosis among the elderly with other chronic medical conditions. *Drugs Aging* **29**, 549–564 (2012).
34. X. Hu *et al.*, MKL1-actin pathway restricts chromatin accessibility and prevents mature pluripotency activation. *Nat. Commun.* **10**, 1695 (2019).
35. N. Tusamda Wakhloo *et al.*, Actomyosin, vimentin and LINC complex pull on osteosarcoma nuclei to deform on micropillar topography. *Biomaterials* **234**, 119746 (2020).
36. B. C. Milon *et al.*, Role of histone deacetylases in gene regulation at nuclear lamina. *PLoS One* **7**, e49692 (2012).
37. A. Malashicheva *et al.*, Various lamin A/C mutations alter expression profile of mesenchymal stem cells in mutation specific manner. *Mol. Genet. Metab.* **115**, 118–127 (2015).

38. E. Mattioli *et al*., Altered modulation of lamin A/C-HDAC2 interaction and p21 expression during oxidative stress response in HGPS. *Aging Cell* **17**, e12824 (2018).
39. J. Shen *et al*., Transcriptional induction of the osteocalcin gene during osteoblast differentiation involves acetylation of histones h3 and h4. *Mol. Endocrinol.* **17**, 743–756 (2003).
40. W. Li *et al*., Decreased bone formation and osteopenia in Lamin A/C-deficient mice. *PLoS One* **6**, e19313 (2011).
41. C. Seeliger *et al*., Five freely circulating miRNAs and bone tissue miRNAs are associated with osteoporotic fractures. *J. Bone Miner. Res.* **29**, 1718–1728 (2014).
42. J. Huang *et al*., The microRNAs miR-204 and miR-211 maintain joint homeostasis and protect against osteoarthritis progression. *Nat. Commun.* **10**, 2876 (2019).
43. J. Delgado-Calle *et al*., Genome-wide profiling of bone reveals differentially methylated regions in osteoporosis and osteoarthritis. *Arthritis Rheum.* **65**, 197–205 (2013).
44. M. A. Jeffries *et al*., Genome-wide DNA methylation study identifies significant epigenomic changes in osteoarthritic cartilage. *Arthritis Rheumatol.* **66**, 2804–2815 (2014).
45. J. C. Crockett, M. J. Rogers, F. P. Coxon, L. J. Hocking, M. H. Helfrich, Bone remodelling at a glance. *J. Cell Sci.* **124**, 991–998 (2011).
46. S. Barreto *et al*., Identification of the mechanisms by which age alters the mechanosensitivity of mesenchymal stromal cells on substrates of differing stiffness: Implications for osteogenesis and angiogenesis. *Acta Biomater.* **53**, 59–69 (2017).
47. T. H. Lin *et al*., Decreased osteogenesis in mesenchymal stem cells derived from the aged mouse is associated with enhanced NF-κB activity. *J. Orthop. Res.* **35**, 281–288 (2017).
48. T. E. Brown, I. A. Marozas, K. S. Anseth, Amplified photodegradation of cell-laden hydrogels via an addition-fragmentation chain transfer reaction. *Adv. Mater.* **29**, 1605001 (2017).
49. A. M. Rosales, K. M. Mabry, E. M. Nehls, K. S. Anseth, Photoresponsive elastic properties of azobenzene-containing poly(ethylene-glycol)-based hydrogels. *Biomacromolecules* **16**, 798–806 (2015).
50. H. Ma, A. R. Killaars, F. W. DelRio, C. Yang, K. S. Anseth, Myofibroblastic activation of valvular interstitial cells is modulated by spatial variations in matrix elasticity and its organization. *Biomaterials* **131**, 131–144 (2017).
51. K. A. Günay *et al*., PEG-anthracene hydrogels as an on-demand stiffening matrix to study mechanobiology. *Angew. Chem. Int. Ed. Engl.* **58**, 9912–9916 (2019).
52. C. Crocini, C. J. Walker, K. S. Anseth, L. A. Leinwand, Three-dimensional encapsulation of adult mouse cardiomyocytes in hydrogels with tunable stiffness. *Prog. Biophys. Mol. Biol.* **154**, 71–79 (2019).
53. R. L. McIntyre, E. G. Daniels, M. Molenaars, R. H. Houtkooper, G. E. Janssens, From molecular promise to preclinical results: HDAC inhibitors in the race for healthy aging drugs. *EMBO Mol. Med.* **11**, e9854 (2019).
54. X. Lyu, M. Hu, J. Peng, X. Zhang, Y. Y. Sanders, HDAC inhibitors as antifibrotic drugs in cardiac and pulmonary fibrosis. *Ther. Adv. Chronic Dis.*, 2040622319862697 (2019).
55. Y. Shin *et al*., DNMT and HDAC inhibitors modulate MMP-9-dependent H3 N-terminal tail proteolysis and osteoclastogenesis. *Epigenetics Chromatin* **12**, 25 (2019).